

Detectors for High-Speed Photon Counting

Wolfgang Becker, Axel Bergmann

Becker & Hickl GmbH, Berlin, becker@becker-hickl.com, bergmann@becker-hickl.com

Detectors for photon counting must have sufficient gain to deliver a useful output pulse for a single detected photon. The output pulse must be short enough to resolve the individual photons at high count rate, and the transit time jitter in the detector should be small to achieve a good time resolution. A wide variety of commercially available photomultipliers and a few avalanche photodiode detectors meet these general requirements. We discuss the applicability of different detectors to time-correlated photon counting (TCSPC), steady-state photon counting, multichannel-scaling, and fluorescence correlation measurements (FCS).

Photon Counting Techniques

In a detector with a gain of the order of 10^6 to 10^8 and a pulse response width of the order of 1 ns each detected photon yields an output current pulse of some mA peak amplitude. The output signal for a low level signal is then a train of random pulses the density of which represents the light intensity. Therefore, counting the detector pulses within defined time intervals - i.e. photon counting - is the most efficient way to record the light intensity with a high gain detector [1].

Steady State Photon Counting

Simple intensity measurement of slow signals can easily be accomplished by a high-gain detector, a discriminator, and a counter that is read in equidistant time intervals. Simple photon counting heads that are connected to a PC via an RS232 interface can be used to collect light signals with photon rates up to a few 10^6 / s within time intervals from a few ms to minutes or hours.

Gated Photon Counting

Gated Photon Counters use a fast gate in front of the counter. The gate is used to count the photons only within defined, usually short time intervals. Gating in conjunction with pulsed light sources can be used to reduce the effective background count rate or to distinguish between different signal components [2,3]. Several parallel counters with different gates can be used to obtain information about the fluorescence lifetime. This technique is used for lifetime imaging in conjunction with laser scanning microscopes [4,5]. The count rate within the short gating interval can be very high, therefore gated photon counters can have maximum count rates of 800 MHz [2].

Multichannel Scalers

Multichannel scalers - or 'multiscalers' count the photons within subsequent time intervals and store the results in subsequent memory locations of a fast data memory. The general principle is shown in fig. 1.

Each sequence - or sweep - is started by a trigger pulse. Therefore the waveform of repetitive signals can be accumulated over many signal periods. Two versions of multiscalers with different accumulation technique exist. The photons can either be directly counted and accumulated in a large and fast data memory, or the

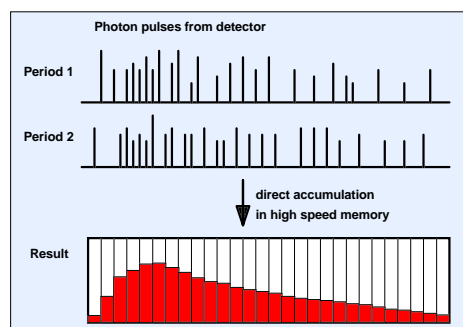


Fig. 1: Multichannel Scaler

detection times of the individual photons are stored in a FIFO memory and the waveform is reconstructed when the measurement is finished. The direct accumulation achieves higher continuous count rates and higher sweep rates, with the FIFO principle it is easier to obtain a short time channel width. Multiscalers for direct accumulation are available with 1ns channel width and 1 GHz continuous count rates [6]. Multiscalers with FIFO principle are available for 500 ps channel width [7]. Unfortunately this is not fast enough for the measurements of fluorescence lifetimes of most organic dyes. However, multiscalers can be an excellent solution for phosphorescence, delayed fluorescence, and luminescence lifetime measurements of inorganic samples. Furthermore, multiscalers are used for LIDAR applications.

The benefits of the multiscaler technique are

- Multiscalers have a near-perfect counting efficiency and therefore achieve optimum signal-to-noise ratio for a given number of detected photons
- Multiscalers are able to record several photons per signal period
- Multiscalers can exploit extremely high detector count rates
- Multiscalers cover extremely long time intervals with high resolution in one sweep

Time-Correlated Single Photon Counting

Time-Correlated Single Photon Counting - or TCSPC - is based on the detection of single photons of a periodical light signal, the measurement of the detection times of the individual photons and the reconstruction of the waveform from the individual time measurements [8,9].

The method makes use of the fact that for low level, high repetition rate signals the light intensity is usually so low that the probability to detect one photon in one signal period is much less than one. Therefore, the detection of several photons can be neglected and the principle shown in fig. 2 right be used:

The detector signal consists of a train of randomly distributed pulses due to the detection of the individual photons. There are many signal periods without photons, other signal periods contain one photon pulse. Periods with more than one photons are very unlikely.

When a photon is detected, the time of the corresponding detector pulse is measured. The events are collected in a memory by adding a '1' in a memory location with an address proportional to the detection time. After many photons, in the memory the histogram of the detection times, i.e. the waveform of the optical pulse builds up. Although this principle looks complicated at first glance, it has a number of striking benefits:

- The time resolution of TCSPC is limited by the transit time spread, not by the width of the output pulse of the detector. With fast MCP PMTs an instrument response width of less than 30 ps is achieved [14,27].

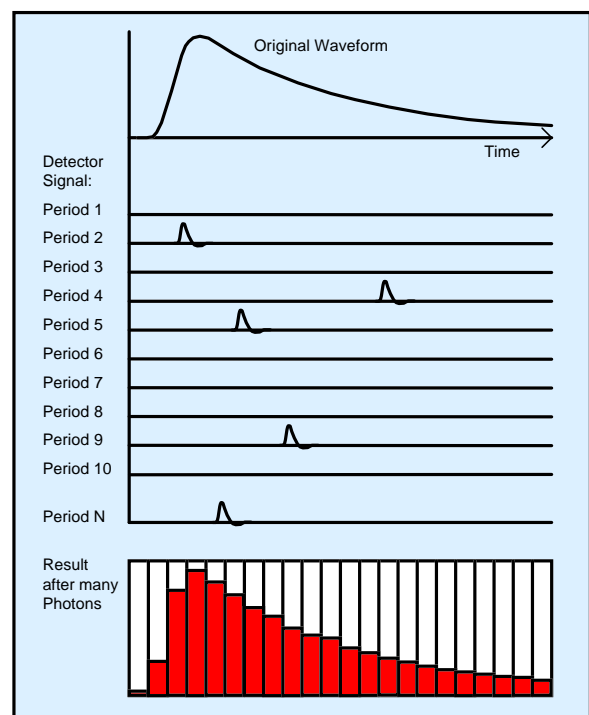


Fig. 2: Principle of the TCSPC technique

- TCSPC has a near-perfect counting efficiency and therefore achieves optimum signal-to-noise ratio for a given number of detected photons [10,11]
- TCSPC is able to record the signals from several detectors simultaneously [9,12-15]
- TCSPC can be combined with a fast scanning technique and therefore be used as a high resolution, high efficiency lifetime imaging (FLIM) technique in confocal and two-photon laser scanning microscopes [9,15,16,18]
- TCSPC is able to acquire fluorescence lifetime and fluorescence correlation data simultaneously [9,17]
- State-of-the-art TCSPC devices achieve count rates in the MHz range and acquisition times down to a few milliseconds [9, 18]

Multi-Detector TCSPC

TCSPC multi-detector operation makes use of the fact that the simultaneous detection of photons in several detector channels is unlikely. Therefore, the single photon pulses from several detector channels - either individual detectors or the anodes of a multi-anode PMT - can be combined in a common timing pulse line. If a photon is detected in one of the channels the pulse is sent through the normal time-measurement circuitry of a single TCSPC channel. In the meantime an array of discriminators connected to the detector outputs generates a data word that indicates in which of the channels the photon was detected. This information is used to store the photons of the individual detector channels in separate blocks of the data memory [9,12-15] (fig. 3).

Multi-detector TCSPC can be used to simultaneously obtain time- and wavelength resolution [15], or to record photons from different locations of a sample [14]. It should be noted that multi-detector TCSPC does not involve any multiplexing or scanning process. Therefore the counting efficiency for each detector channel is still close to one, which means that the efficiency of a multi-detector TCSPC system can be considerably higher of single channel TCSPC device.

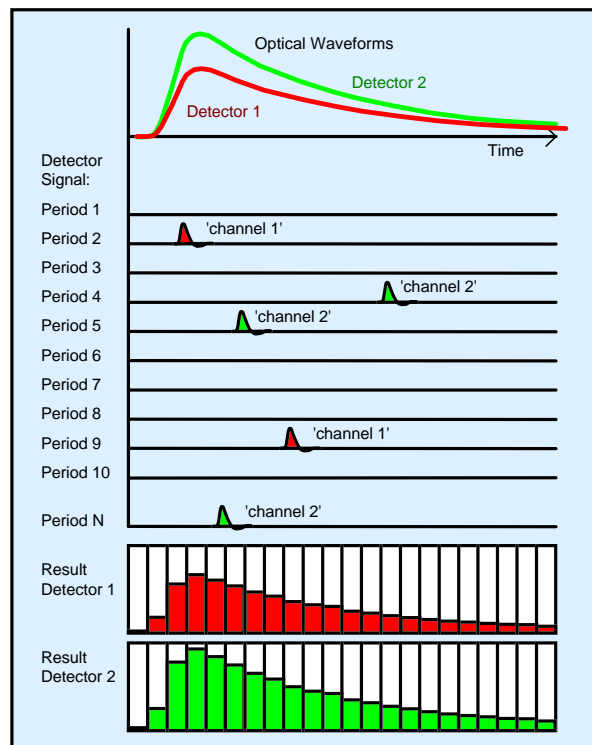


Fig. 3: Multi-detector TCSPC

Photon Counting for Fluorescence Correlation Spectroscopy

Fluorescence Correlation Spectroscopy (FCS) exploits intensity fluctuations in the emission of a small number of chromophore molecules in a femtoliter sample volume [19,20]. The fluorescence correlation spectrum is the autocorrelation function of the intensity fluctuation. FCS yields information about diffusion processes, conformational changes of chromophore - protein complexes and intramolecular dynamics. Fluorescence correlation spectra can be obtained directly by hardware correlators or by recording the detection times of the individual photons and calculating the FCS curves by software. The second technique can be combined with TCSPC to obtain FCS and lifetime data simultaneously. Moreover, the multidetector capability of TCSPC can be used to detect photons in different wavelength intervals or of different polarisation simultaneously [17,21].

The data structure for combined lifetime / FCS data acquisition in the an SPC-830 module [9] is shown in fig. 4. For each detector an individual correlation spectrum and a fluorescence decay curve can be calculated. If several detectors are used to record the photons from different chromophores, the signals of these chromophores can be cross-correlated. The fluorescence cross-correlation spectrum shows whether the molecules of both chromophores and the associated protein structures are linked or diffuse independently.

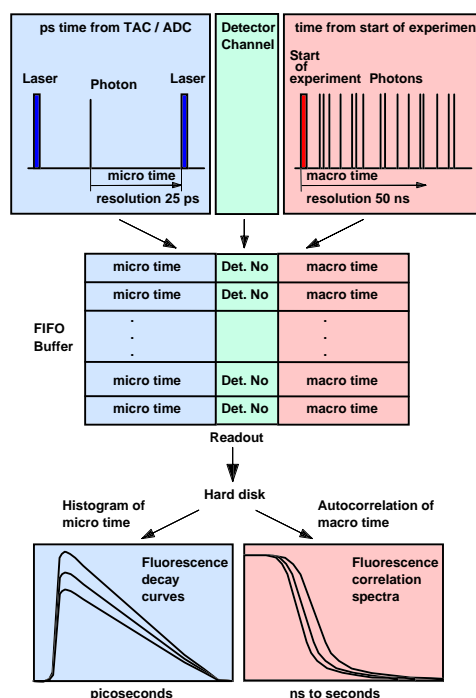


Fig. 4: Simultaneous FCS / lifetime data acquisition

Detector Principles

The most common detectors for low level detection of light are photomultiplier tubes. A conventional photomultiplier tube (PMT) is a vacuum device which contains a photocathode, a number of dynodes (amplifying stages) and an anode which delivers the output signal [1,22].

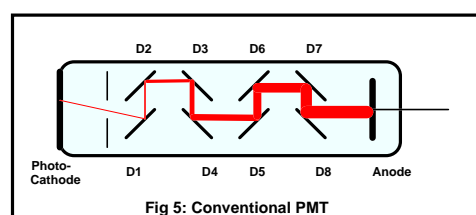


Fig 5: Conventional PMT

The operating voltage builds up an electrical field that accelerates the electrons from the cathode to the first dynode D1, further to the next dynodes, and from D8 to the anode. When a photoelectron emitted by the photocathode hits D1 it releases several secondary electrons. The same happens for the electrons emitted by D1 when they hit D2. The overall gain reaches values of 10^6 to 10^8 . The secondary emission at the dynodes is very fast, therefore the secondary electrons resulting from one photoelectron arrive at the anode within a few ns or less. Due to the high gain and the short response a single photoelectron yields a easily detectable current pulse at the anode.

A wide variety of dynode geometries has been developed [1]. Of special interest for photon counting are the 'linear focused' type dynodes which yield a fast single electron response, and the 'fine mesh' and 'metal channel' type which offer position-sensitivity when used with an array of anodes.

A similar gain effect as in the conventional PMTs is achieved in the Channel PMT (fig 6) and in the Microchannel PMT (Fig. 7, MCP). These detectors use channels with a conductive coating the walls of which work as secondary emission targets [1]. Microchannel PMTs are the fastest photon counting detectors currently available. Moreover, the microchannel plate technique allows to build position-sensitive detectors and image intensifiers.

To obtain position sensitivity, the single anode can be replaced with an array of individual anode elements (fig. 8). By individually detecting the pulses from the anode elements the position of the corresponding photon on the photocathode can be determined. Multi-anode PMTs are particularly interesting in conjunction with time-correlated single photon counting (TCSPC) because this technique is able to process the photon pulses from several detector channels in only one time-measurement channel [9,12-15].

The gain systems used in photomultipliers can also be used to detect electrons or ions. These ‘Electron Multipliers’ are operated in the vacuum, and the particles are fed directly into the dynode system, the multiplier channel or onto the multichannel plate (fig. 9).

Cooled avalanche photodiodes can be used to detect single optical photons if they are operated close to or slightly above the breakdown voltage [23-26] (fig. 10). The generated electron-hole pairs initiate an avalanche breakdown in the diode. Active or passive quenching circuits must be used to restore normal operation after each photon. Single-photon avalanche photodiodes (SPADs) have a high quantum efficiency in the visible and near-infrared range.

X ray photons can be detected by PIN diodes. A single high energy X ray photon generates so many electron-hole pairs in the diode so that the resulting charge pulse can be detected by an ultra-sensitive charge amplifier. However, due to the limited speed of the amplifier these detectors have a time resolution in the us range and do not reach high count rates. They can, however, distinguish photons of different energy by the amount of charge generated.

Detector Parameters

Single Electron Response

The output pulse of a detector for a single photoelectron is called the ‘Single Electron Response’ or ‘SER’. Some typical SER shapes for PMTs are shown in fig. 11.

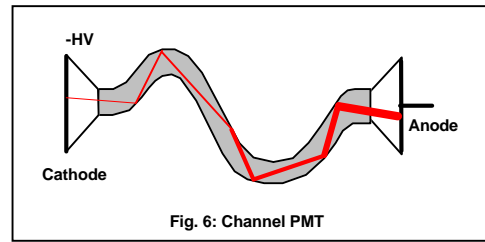


Fig. 6: Channel PMT

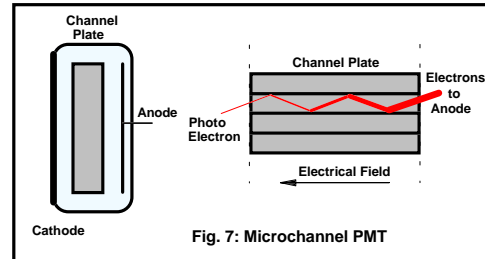


Fig. 7: Microchannel PMT

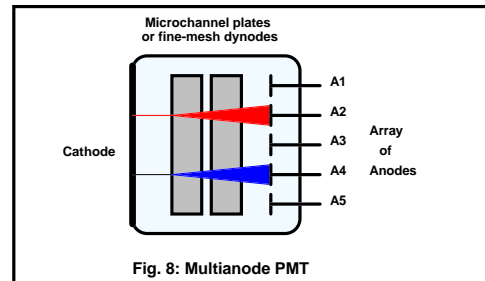


Fig. 8: Multianode PMT

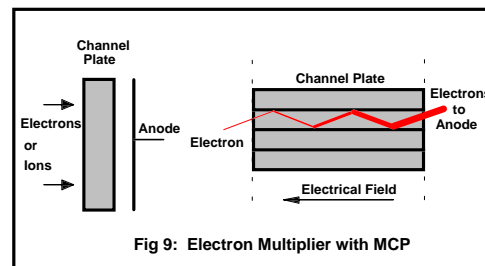


Fig 9: Electron Multiplier with MCP

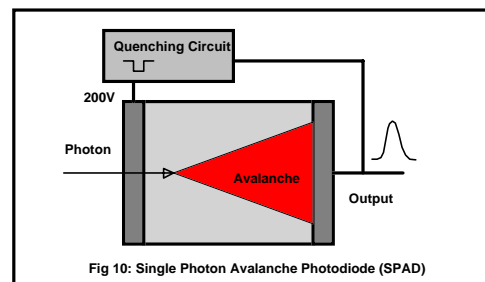


Fig 10: Single Photon Avalanche Photodiode (SPAD)

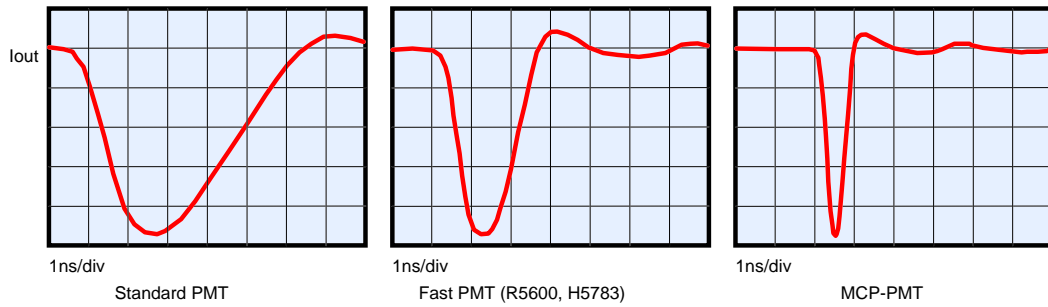


Fig. 11: Single electron response (SER) of different photomultipliers

Due to the random nature of the detector gain, the pulse amplitude varies from pulse to pulse. The pulse height distribution can be very broad, up to 1:5 to 1:10. Fig. 12 shows the SER pulses of an R5600 PMT recorded by a 400 MHz oscilloscope.

The following considerations are made with G being the average gain, and I_{SER} being the average peak current of the SER pulses.

The peak current of the SER is approximately

$$I_{SER} = \frac{G \cdot e}{FWHM} \quad (G = \text{PMT Gain}, e = 1.6 \cdot 10^{-19} \text{ As}, FWHM = \text{SER pulse width, full width at half maximum})$$

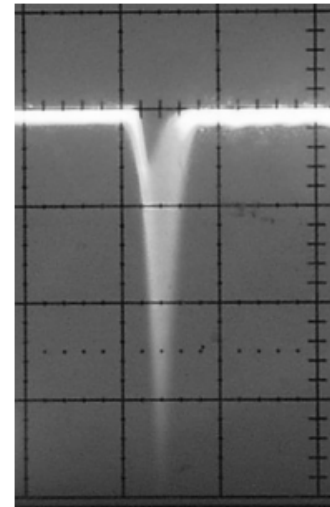


Fig. 12: Amplitude jitter of SER pulses

The table below shows some typical values. I_{SER} is the average SER peak current and V_{SER} the average SER peak voltage when the output is terminated with 50Ω . I_{max} is the maximum permitted continuous output current of the PMT.

PMT	PMT Gain	FWHM	I_{SER}	$V_{SER} (50 \Omega)$	$I_{max} (\text{cont})$
Standard	10^7	5 ns	0.32 mA	16 mV	100uA
Fast PMT	10^7	1.5 ns	1 mA	50 mV	100uA
MCP PMT	10^6	0.36 ns	0.5mA	25 mV	0.1uA

There is one significant conclusion from this table: If the PMT is operated near its full gain the peak current I_{SER} from a single photon is much greater than the maximum continuous output current. Consequently, for steady state operation the PMT delivers a train of random pulses rather than a continuous signal. Because each pulse represents the detection of an individual photon the pulse density - not the pulse amplitude - is a measure of the light intensity at the cathode of the PMT [1,2,3,6].

Obviously, the pulse density is measured best by counting the PMT pulses within subsequent time intervals. Therefore, photon counting is a logical consequence of the high gain and the high speed of photomultipliers.

Transit Time Spread and Timing Jitter

The delay between the absorption of a photon at the photocathode and the output pulse from the anode of a PMT varies from photon to photon. The effect is called ‘transit time spread’, or TTS. There are three major TTS components in conventional PMTs and MCP PMTs - the emission at the photocathode, the multiplication process in the dynode system or microchannel plate, and the timing jitter of the subsequent electronics.

The time constant of the photoelectron emission at a traditional photocathodes is small compared to the other TTS components and usually does not noticeably contribute to the transit time spread. However, high efficiency semiconductor-type photocathodes (GaAs, GaAsP, InGaAs) are much slower and can introduce a transit time spread of the order of 100 to 150 ps. Moreover, photoelectrons are emitted at the photocathode of a photomultiplier at random locations, with random velocities and in random directions. Therefore, the time they need to reach the first dynode or the channel plate is slightly different for each photoelectron (fig. 13). Since the average initial velocity of a photoelectron increases with decreasing wavelength of the absorbed photon the transit-time spread is wavelength-dependent.

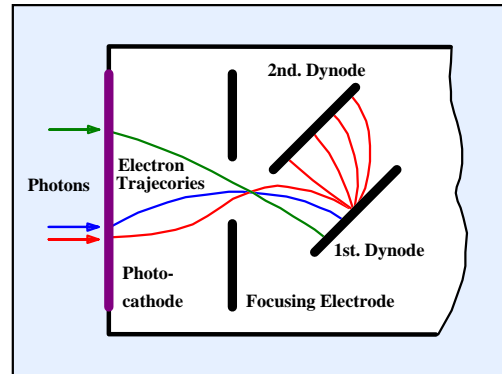


Fig. 13: Different electron trajectories cause different transit times in a PMT

As the photoelectrons at the cathode, the secondary electrons emitted at the first dynodes of a PMT or in the channel plate of an MCP PMT have a wide range of start velocities and start in any direction. The variable time they need to reach the next dynode adds to the transit time spread of the PMT.

Another source of timing uncertainty is the timing jitter in the discriminator at the input of a photon counter. The amplitude of the single electron pulses at the output of a PMT varies, which causes a variable delay in the trigger circuitry. Although timing jitter due to amplitude fluctuations can be minimised by constant fraction discriminators it cannot be absolutely avoided. Electronic timing jitter is not actually a property of the detector, but usually cannot be distinguished from the detector TTS.

TTS does exist also in single-photon avalanche photodiodes. The reason of TTS in SPADs is the different depth in which the photons are absorbed. This results in different conditions for the build-up of the carrier avalanche and in different avalanche transit times. Consequently the TTS depends on the wavelength. Moreover, if a passive quenching circuit is used, the reverse voltage may not have completely recovered from the breakdown of the previous photon. The result is an increase or shift of the TTS with the count rate.

The TTS of a PMT is usually much shorter than the SER pulse width. In linear applications where the time resolution is limited by the SER pulse width the TTS is not important. The resolution of photon counting, however, is not limited by the SER pulse width. Therefore, the TTS is the limiting parameter for the time resolution of photon counting.

Cathode Efficiency

The efficiency, i.e. the probability that a particular photon causes a pulse at the output of the PMT, depends on the efficiency of the photocathode. Unfortunately the sensitivity S of a

photocathode is usually not given in units of quantum efficiency but in mA of photocurrent per Watt incident power. The quantum efficiency QE is

$$QE = S \frac{h c}{e \lambda} = \frac{S}{\lambda} \cdot 1.24 \cdot 10^6 \frac{W m}{A}$$

The efficiency for the commonly used photocathodes is shown in fig. 14. The QE of the conventional bialkali and multialkali cathodes reaches 20 to 25 % between 400 and 500 nm. The recently developed GaAsP cathode reaches 45 %. The GaAs cathode has an improved red sensitivity and is a good replacement for the multialkali cathode above 600 nm.

Generally, there is no significant difference between the efficiency of similar photocathodes in different PMTs and from different manufacturers. The differences are of the same order as the variation between different tube of the same type. Reflection type cathodes are a bit more efficient than transmission type photocathodes. However, reflection type photocathodes have non-uniform photoelectron transit times to the dynode system and therefore cannot be used in ultra-fast PMTs. A good overview about the characteristics of PMTs is given in [1].

The typical efficiency of the Perkin Elmer SPCM-AQR single photon avalanche photodiode (SPAD) modules is shown in the figure right (after [24]). The wavelength dependence follows the typical curve of a silicon photodiode and reaches more than 70% at 700nm. However, the active area of the SPCM-AQR is only 0.18 mm wide, and diodes with much smaller areas have been manufactured [23]. Therefore the high efficiency of an SPAPD can only be exploited if the light can be concentrated to such a small area.

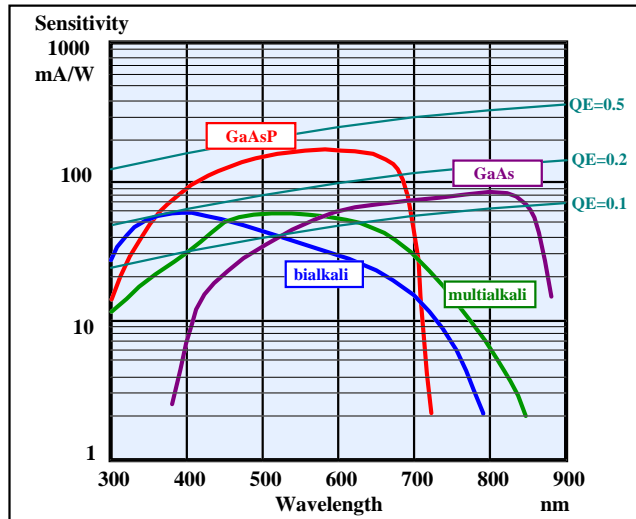


Fig. 14: Sensitivity of different photocathodes [1]

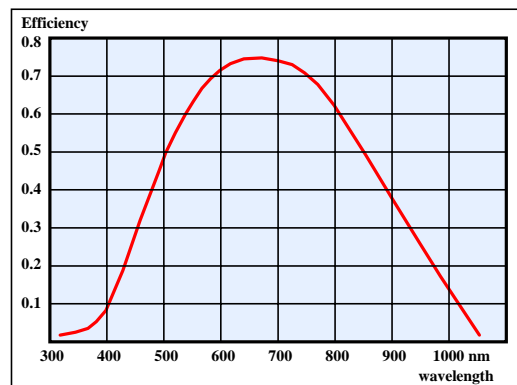


Fig. 15: Quantum efficiency vs. wavelength for SPAD. Perkin-Elmer SPCM-AQR module [24]

Pulse Height Distribution

The single photon pulses obtained from PMTs and MCPs have a considerable amplitude jitter. A typical pulse amplitude distribution of a PMT is shown in fig. 16. The amplitude spectrum shows a more or less pronounced peak for the photon pulses and a continuous increase of the background at low amplitudes. The background originates from thermal emission of electrons in the dynode systems, from noise of preamplifiers, and from noise pickup from the environment. The amplitude of the single photon pulses can vary by a factor of 10 and more.

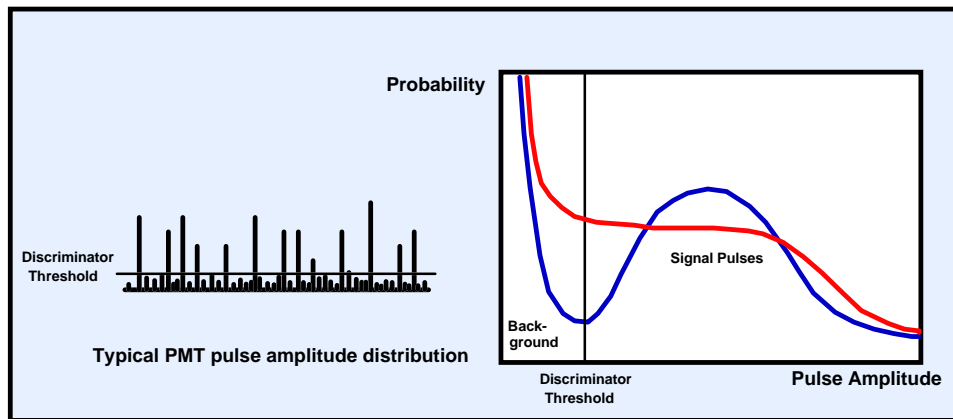


Fig 16: Pulse height distribution of a PMT and discriminator threshold for optimum counting performance

In good PMTs and MCPs the single photon pulse amplitudes should be clearly distinguished from the background noise. Then, by appropriate setting the discriminator threshold of the photon counter, the background can be effectively suppressed. If the photon pulses and the background are not clearly distinguished either the background cannot be efficiently suppressed or a large fraction of the photon pulses is lost. Therefore, next to a high QE of the cathode, a good pulse height distribution is essential to get a high counting efficiency.

The pulse height distribution has also noticeable influence on the time resolution obtained in TCSPC applications. Of course, a low timing jitter can only be achieved if the amplitude of single photon pulses is clearly above the background noise level.

The pulse height distribution of the same PMT type can differ considerably for different cathode versions. The bialkali versions are usually the best, multialkali is mediocre and extended multialkali (S25) can be disastrous. The reason might be that during the cathode formation cathode material is spilled into the dynode system or that the cathode material is also used for coating the dynodes.

Dark Count Rate

The dark count rate of a PMT depends on the cathode type, the cathode area, and the temperature. The dark count rate is highest for cathodes with high sensitivity at long wavelengths. Depending on the cathode type, there is an increase of a factor of 3 to 10 for a 10 °C increase in temperature. Therefore, additional heating, i.e. by the voltage divider resistors, amplifiers connected to the output, or by the coils of shutters should be avoided. The most

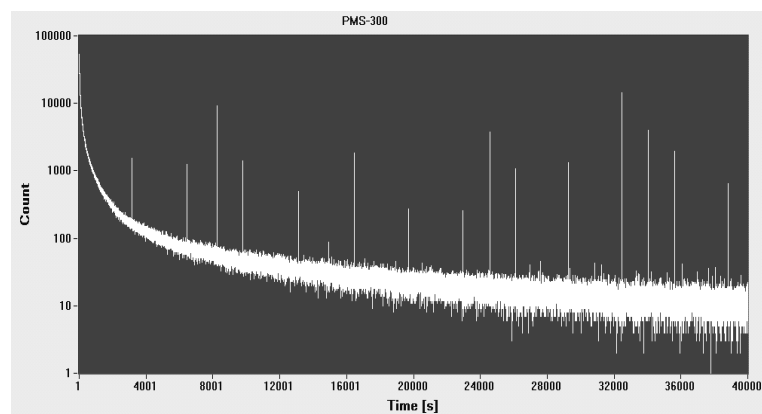


Fig.17: Decrease of dark count rate (counts per second) of a H5773P-01 after exposing the cathode to room light. The device was cooled to 5°C. The peaks are caused by scintillation effects.

efficient way to keep the dark count rate low is thermoelectric cooling. Exposing the cathode of a switched-off PMT to daylight increases the dark count rate considerably. For the traditional cathodes the effect is reversible, but full recovery takes several hours, see fig. 17. Semiconductor cathodes should not be exposed to full daylight at all.

After extreme overload, e.g. daylight on the cathode of an operating PMT, the dark count rate is permanently increased by several orders of magnitude. The tube is then damaged and does not recover.

Many PMTs produce random single pulses of extremely high amplitude or bursts of pulses with extremely high count rate. Such bursts are responsible for the peaks in fig. 17. The pulses can originate from scintillation effects by radioactive decay in the vicinity of the tube, in the tube structure itself, by cosmic ray particles or from tiny electrical discharges in the cathode region. Therefore not only the tube, but also the materials in the cathode region must be suspected to be the source of the effect. Generally, there should be some mm clearance around the cathode region of the tube.

Afterpulses

Most detectors have an increased probability to produce a dark count pulse in a time interval of some 100 ns to some μs after the detection of a photon. Afterpulses can be caused by ion feedback, or by luminescence of the dynode material and the glass of the tube. They are detectable in almost any conventional PMT. Afterpulsing of an R5600 tube is shown in fig. 18.

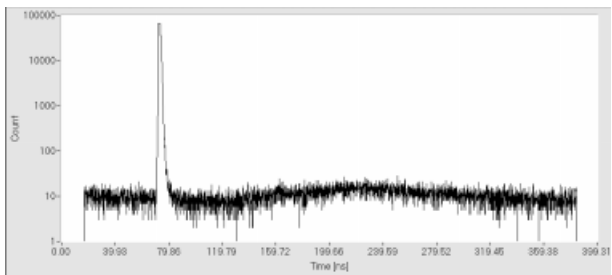
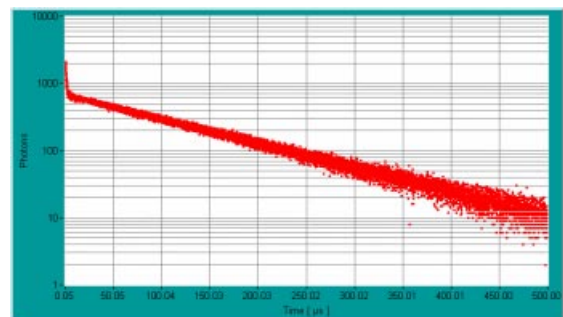


Fig. 18: Afterpulsing in an R5600 PMT tube. TCSPC measurement with Becker & Hickl SPC-630. The peak is the laser pulse, afterpulses cause a bump 200 ns later

Afterpulsing can be a problem in high repetition rate TCSPC applications, particularly with titanium-sapphire lasers or diode lasers, and in fluorescence correlation experiments. At high repetition rate the afterpulses from many signal periods accumulate and cause an appreciable signal-dependent background. Correlation spectra can be severely distorted by afterpulsing.

Afterpulsing shows up most clearly in histograms of the time differences between subsequent photons or in correlation spectra. For classic light, i.e. from an incandescent lamp, the histogram of the time differences drops exponentially with the time difference. Any deviation from the exponential drop indicates correlation between the detection events, i.e. non-ideal behaviour of the detector. Afterpulses show up as a peak centred at the average time difference of primary pulses and afterpulses.



A correlation spectrum is the autocorrelation function of the photon density versus time. Classic light delivers a constant background of random coincidences of the detection events. As in the histogram of time differences, afterpulses show up as a peak centred at the average time difference of primary pulses and afterpulses.

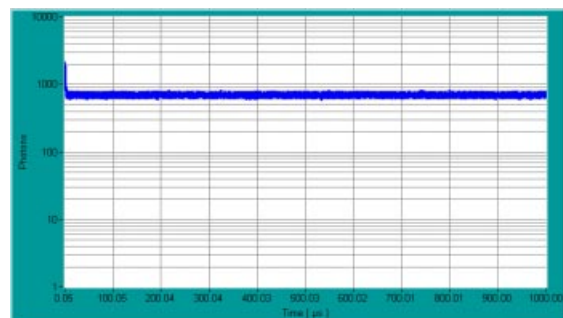


Fig. 19: Histogram of times between photons (top) and correlation spectrum (bottom) for classic light. The peak at short times is due to afterpulsing.

Typical curves for a traditional R932 PMT are shown in fig. 19.

Photon Counting Performance of Selected Detectors

R3809U MCP-PMT

The TCSPC system response for a Hamamatsu R3809U-50 MCP [27] is shown in fig. 20. The MCP was illuminated with a femtosecond Ti:Sa laser, the response was measured with an SPC-630 TCSPC module. A HFAC-26-01 preamplifier was used in front of the SPC-630 CFD input. At an operating voltage of -3 kV the FWHM (full width at half maximum) of the response is 28 ps.

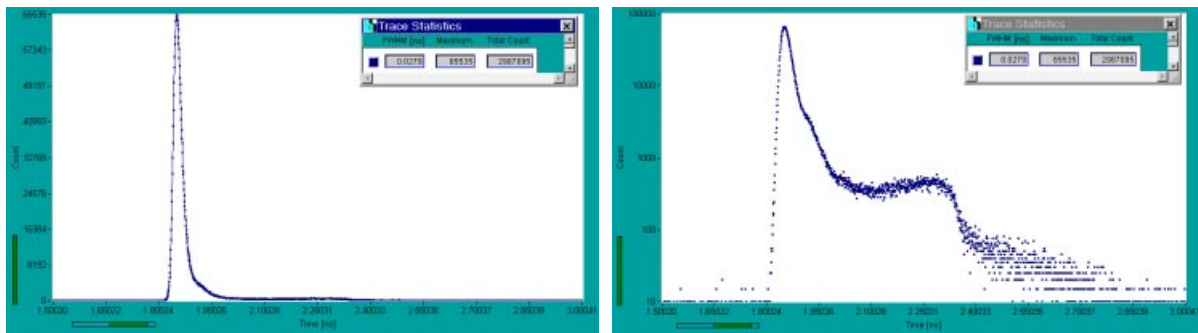


Fig. 20: R3809U, TCSPC instrument response. Operating voltage-3kV, preamplifier gain 20dB, discriminator threshold - 80mV

The response has a shoulder of some 400 ps duration and about 1% of the peak amplitude. This shoulder seems to be a general property of all MCPs and appears in all of these devices.

The width of the response can be reduced to 25 ps by increasing the operating voltage to the maximum permitted value of -3.4 kV. However, for most applications this is not recommended for the following reason:

As all MCP-PMTs, the R3809U allows only a very small maximum output current. This sets a limit to the maximum count rate that can be obtained from the device. The maximum count rate depends on the MCP gain, i.e. of the supply voltage. The count rate for the maximum output current of 100 nA as a function of the supply voltage is shown in fig. 21.

To keep the counting efficiency constant the CFD threshold was adjusted to get a constant count rate at a reference intensity that gave 20,000 counts per second. Fig. 21 shows that count rates in excess of 2 MHz can be reached.

The R3809U tubes have a relatively good SER pulse height distribution which seems to be independent of the cathode type - possibly a result of the independent manufacturing of the channel plate and the cathode. Therefore a good counting efficiency can be achieved.

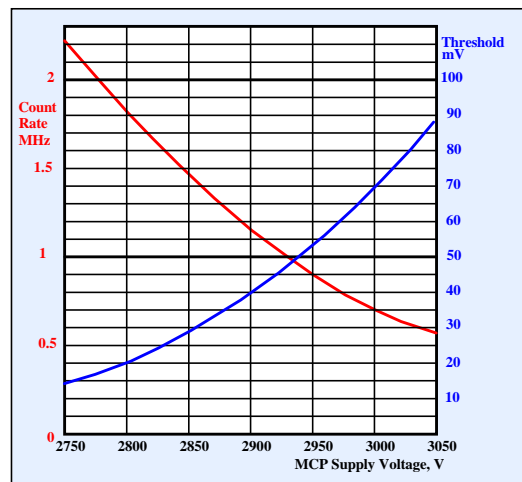


Fig. 21: R3809U, count rate for 100 nA anode current and optimum discriminator threshold vs. supply voltage. HFAC-26-01 (20dB) preamplifier

Fig. 22 shows the histogram of the time intervals between the recorded photons. The count rate was about 10,000 photons per second, the data were obtained with an SPC-830 in the 'FIFO' mode. Interestingly, the R3809U is free of afterpulsing.

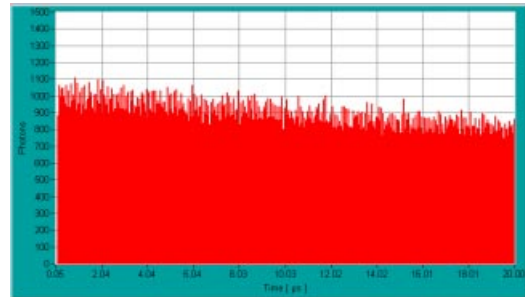


Fig. 22: R3809U, histogram of times between photons. No afterpulses are detected.

Due to the short TCSPC response and the absence of afterpulses the R3809U is an ideal detector for TCSPC fluorescence lifetime measurements, for TCSPC lifetime imaging, and for combined lifetime / FCS or other correlation experiments. Recently Hamamatsu announced the R3809U MCP with GaAs, GaAsP, and infrared cathodes for up to 1700 nm. Although these MCPs are not as fast as the versions with conventional cathodes they might be the ultimate detectors for combined FCS / lifetime experiments.

The flipside is that MCPs are expensive and can easily be damaged by overload. Therefore the R3809U should be operated with a preamplifier that monitors the output current. If overload conditions are to be expected, i.e. by the halogen or mercury lamp of a scanning microscope, electronically driven shutters should be used and high voltage shutdown should be accomplished to protect the detector.

H7422

The H7422 incorporates a GaAs or GaAsP cathode PMT, a thermoelectric cooler, and the high voltage power supply [28]. Hamamatsu delivers a small OEM power supply to drive the cooler. However, we could not use this power supply because it generated so much noise that photon counting with the H7422 was not possible. Furthermore, we found that the H7422 shuts down if the gain control voltage is changed faster than about 0.1V / s. Apparently fast changes activate an internal overload shutdown. Unfortunately the device can only be re-activated by cycling the +12 V power supply.

Therefore we use the Becker & Hickl DCC-100 detector controller. It drives the cooler and supplies the +12 V and a software-controlled gain control voltage to the H7422. Furthermore, the DCC in conjunction with a HFAC-26-1 preamplifier can be connected to shut down the gain of the H7422 on overload. If the H7422 shuts down internally for any reason, cycling the +12 V is only a mouse click into the DCC-100 operating panel.

The TCSPC system response of an H7422-40 is shown in Fig. 23.

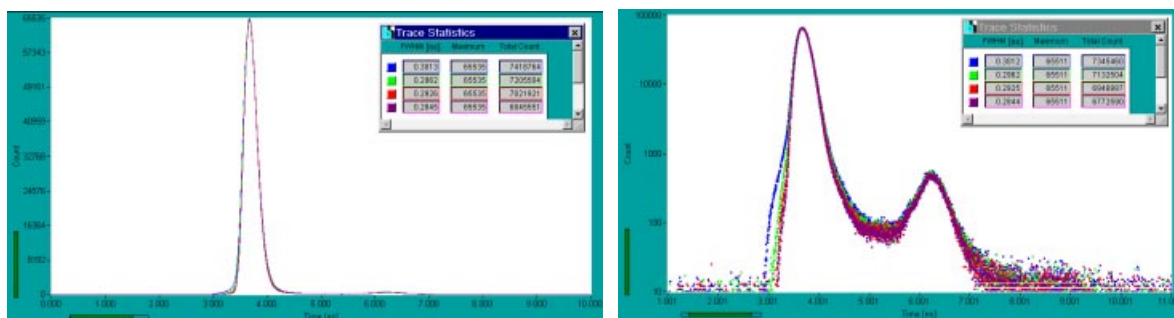


Fig. 23: H7422-40, TCSPC Instrument response function. Gain control voltage 0.9V (maximum gain), preamplifier 20dB, discriminator threshold -200mV, -300mV, -400mV and -500mV

The FWHM of the system response is about 300 ps. There is a weak secondary peak about 2.5 ns after the main peak, and a peak prior to the main peak can appear at low discriminator thresholds. The width of the response does not depend appreciably of the discriminator threshold. This is an indication that the response is limited by the intrinsic speed of the semiconductor photocathode.

The afterpulsing probability of the H7422-40 can be seen from the histogram of the time intervals of the photon (fig. 24). For maximum gain the afterpulse probability in the first 1.5 μ s is very high (fig. 24, red curve, control voltage 0.9V). If the gain is reduced the afterpulse probability decreases considerably (fig. 24, blue curve, 0.63V). The timing resolution does not decrease appreciably at the reduced gain, fig. 25.

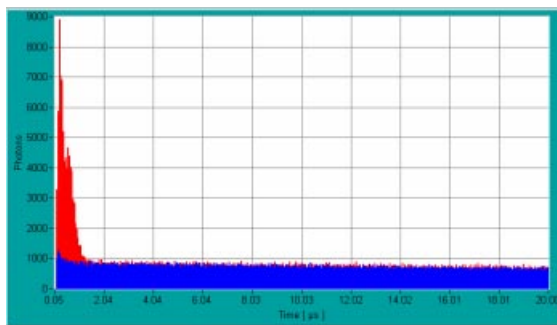


Fig. 24: H7422-40, histogram of times between photons. Gain control voltage 0.9V (red) and 0.63V (blue). Afterpulse probability increases with gain.

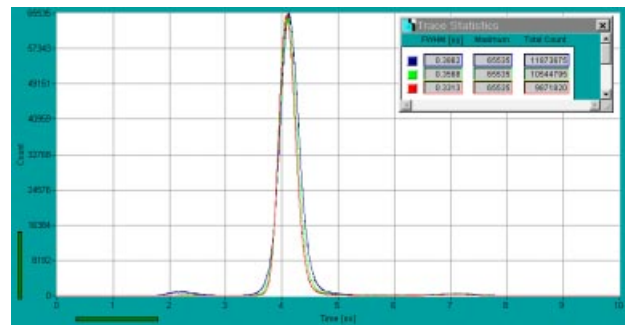


Fig. 25: H7422-40, TCSPC Instrument response function. Gain control voltage 0.63V, preamplifier 20dB, discriminator threshold -30mV, -50mV, -70mV

The H7422 is a good detector for TCSPC applications when sensitivity has a higher priority than time resolution. A typical application is TCSPC imaging with laser scanning microscopes [18,29]. The high quantum efficiency helps to reduce photobleaching which is the biggest enemy of lifetime imaging in scanning microscopes.

The H7422 can also be used to investigate diffusion processes in cells or conformational changes of dye / protein complexes by combined FCS / lifetime spectroscopy. Although the accuracy in the time range below 1.5 μ s is impaired by afterpulsing, processes at longer time scales can be efficiently recorded.

Another application of the H7422 is optical tomography with pulses NIR lasers. Because the measurements are run in-vivo it is essential to acquire a large number of photons in a short measurement time. Particularly in the wavelength range above 800 nm the efficiency of H7422-50 and -60 yields a considerable improvement compared to PMTs with conventional cathodes.

H7421

The Hamamatsu H7421 is similar to the H7422 in that it contains a GaAs or GaAsP cathode PMT, a thermoelectric cooler, and the high voltage power supply. However, the output of the PMT is connected to a discriminator that delivers TTL pulses. The output of the PMT is not directly available, and the PMT gain and the discriminator threshold cannot be changed. The module is therefore easy to use. However, because the discriminator is not of the constant fraction type, the TCSPC timing performance is by far not as good as for the H7422, see figure 26.

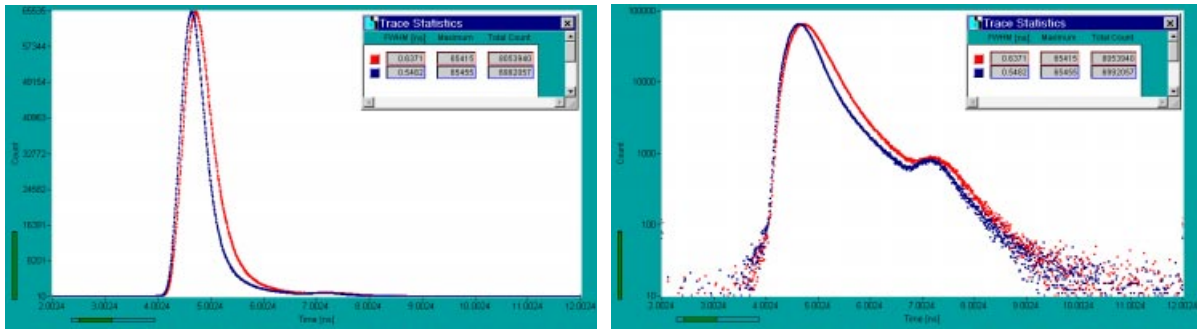


Fig. 26: H7422-50, TCSPC response function for a count rate of 30 kHz (blue) and 600 kHz (red)

The FWHM is only 600 ps. Moreover, it increases for count rates above some 100 kHz. Interestingly no such count rate dependence was found for the H7422. Obviously the H7422 is a better solution if high time resolution and high peak count rate is an issue.

H5783 and H5773 Photosensor Modules, PMH-100

The H5783 and H5773 photosensor modules contain a small (TO9 size) PMT and the high voltage power supply [30]. They come in different cathode and window versions. A ‘P’ version selected for good pulse height distribution is available for the bialkali and multialkali tubes. The typical TCSPC response of a H5773P-0 is shown in fig. 27. The device was tested with a 650 nm diode laser of 80 ps pulse width. A HFAC-26-10 preamplifier was used, and the response was recorded with an SPC-730 TCSPC module.

The response function has a pre-peak about 1 ns before the main peak and an secondary peak 2 ns after. The pre-peak is caused by low amplitude pulses, probably from photoemission at the first dynode. It can be suppressed by properly adjusting the discriminator threshold. The secondary peak is independent of the discriminator threshold.

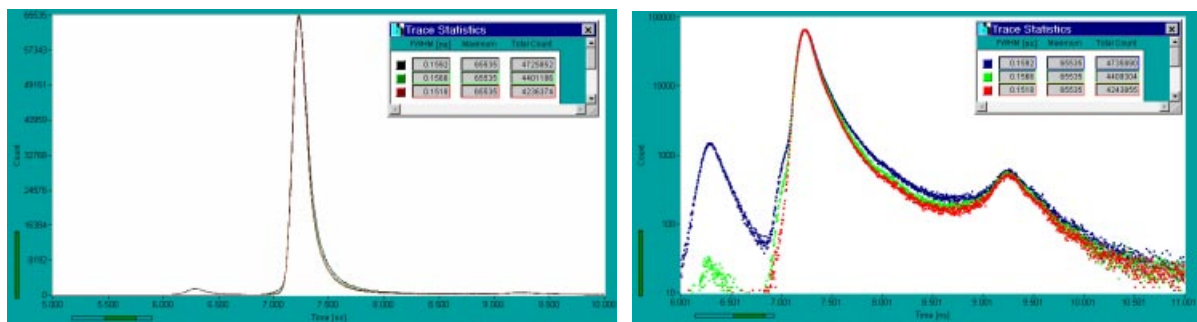


Fig. 27: H5773P-0, TCSPC instrument response. Maximum gain, preamplifier gain 20dB, discriminator threshold -100mV, -300mV and -500mV

The Becker & Hickl PMH-100 module contains a H5773P module, a 20 dB preamplifier, and an overload indicator. The response is the same as for the H5773P and a HFAC-26 amplifier. However, because the PMT and the preamplifier are in the same housing, the PMH-100 has a superior noise immunity. This results in an exceptionally low differential nonlinearity in TCSPC measurements.

A histogram of the times between the photon pulses for the H5773 is shown in fig. 28. The devices show relatively strong afterpulsing, particularly the multialkali (-1) tubes.

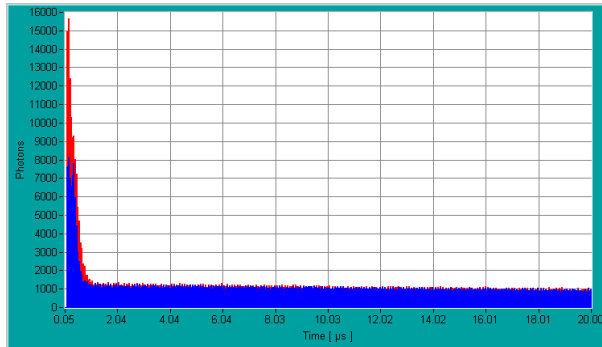


Fig. 28: Histogram of times between photons for H5773P-0 (blue) and H5773P-1 (red). The afterpulse probability is higher for the -1 version

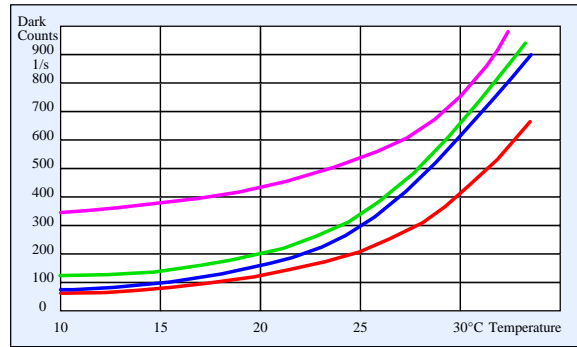


Fig. 29: Dark count rate for different H5773P-01 modules

Fig. 29 shows the dark count rate for different H5773P-1 modules as a function of ambient temperature. Taking into regards the small cathode area of the devices the dark count rates are relatively high. Selected devices with lower dark count rate are available.

The H5783, the H5773 and particularly the PMH-100 are easy to use, rugged and fast detectors that can be used for TCSPC, multiscalers and gated photon counting as well. In multiscaler applications the detectors reach peak count rates of more that 150 MHz for a few 100 ns. The detectors are not suitable for FCS or similar correlation experiments on the time scale below 1 us.

R7400 and R5600 TO-8 PMTs

The R7400 and the older R5600 are bare tubes similar to that used in the H5783 and H5773. There is actually no reason to use the bare tubes instead of the complete photosensor module. However, for the bare tube the voltage divider can be optimised for smaller TTS or improved linearity at high count rate. The TTS width decreases with the square root of the voltage between the cathode and the first dynode. It is unknown how far the voltage can be increased without damage. A test tube worked stable at 1 kV overall voltage with a three-fold increase of the cathode-dynode voltage. The decrease of the response width is shown in fig. 30.

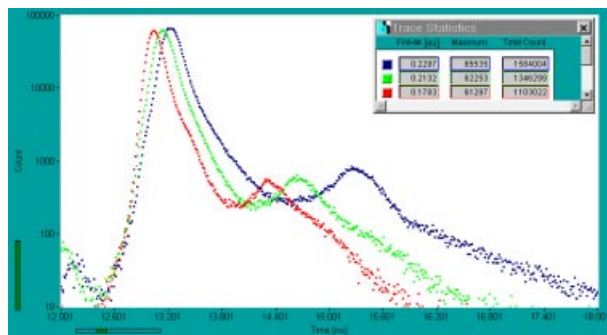


Fig. 30: R5900P-1, -1kV supply voltage: TCSPC response for different voltage between cathode and first dynode. Blue, green and red: 1, 2 and 3 times nominal voltage

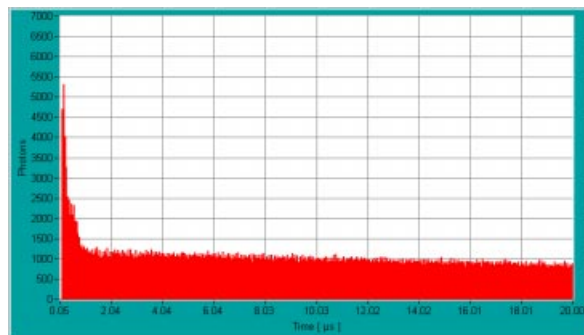


Fig. 31: H5773P-1, -1kV : Histogram of times between photons.

The afterpulse probability is the same as for the H5783 and H5773 photosensor modules (fig. 31).

It is questionable whether the benefit of a slightly shorter response compensates for the inconvenience of building a voltage divider and using a high voltage power supply. However, if a large number of tubes has to be used, i.e. in an optical tomography setup, using the R5600 or R7400 can be reasonable.

R5900-L16 Multichannel PMT and PML-16 Multichannel Detector Head

The Hamamatsu R5900-L16 is a multi-anode PMT with 16 channels in a linear arrangement. In conjunction with a polychromator the detector can be used for multi-wavelength detection. If the R5900-L16 is used with steady-state and gated photon counters or with multiscalers 16 parallel recording channels, e.g. two parallel Becker & Hickl PMM-328 modules are required. For TCSPC application the multi-detector technique described in [9] and [12-15] can be used. TCSPC multi-detector operation is achieved by combining the photon pulses of all detector channels into one common timing pulse line and generating a ‘channel’ signal which indicates in which of the PMT channels a photon was detected. The Becker & Hickl PML-16 detector head [13] contains the R5900-L16 tube and all the required electronics.

The R5900-L16 has also been used with a separate routing device [12,31]. However, in a setup like this noise pick-up from the environment and noise from matching resistors and preamplifiers adds up so that the timing performance is sub-optimal.

The TCSPC response of two selected channels of the PML-16 detector head is shown in fig. 32. The response of a single channel of different R5900-L16 is between 150 ps and 220 ps FWHM.

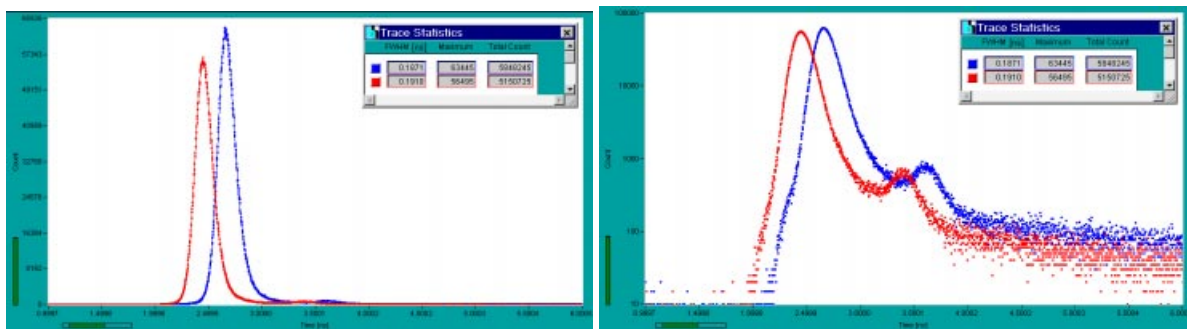


Fig. 32: System response of two selected channels of the PML-16 detector head

The response is slightly different for the individual channels. Fig. 33 shows the response for the 16 channels as sequence of curves and as a colour-intensity plot. There is a systematic wobble in the delay of response with the channel number. That means, for the analysis of fluorescence lifetime measurements the instrument response function (IRF) must be measured for all channels, and each channel must be de-convoluted with its individual IRF.

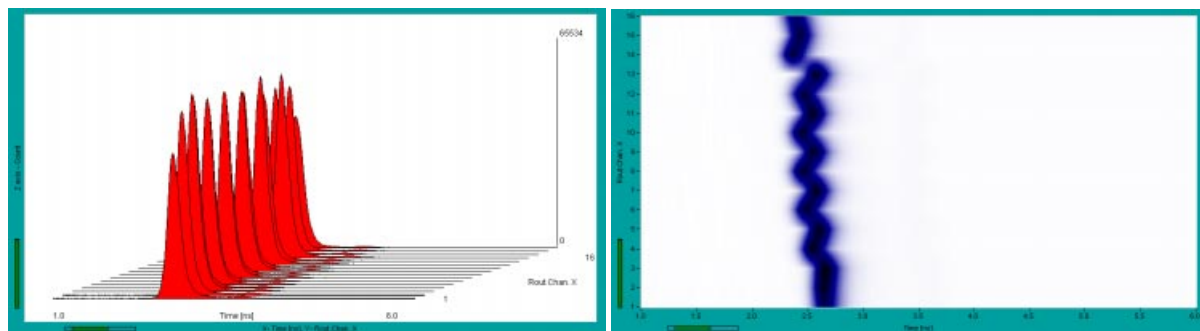


Fig. 33: System response of the PML-16 / R5900-L16 channels. Left curve plot, right colour-intensity plot

The data sheet of the R5900-L16 gives a channel crosstalk of only 3%. There is certainly no reason to doubt about this value. However, in real setup it is almost impossible to reach such a small crosstalk. If crosstalk is an issue the solution is to use only each second channel of the R5900-L16 [31]. If the PML-16 is used with only 8 channels, the data of the unused channels should simply remain unused. If the R5900-L16 is used outside the PML-16 the unused anodes should be terminated into ground with 50 Ω .

A histogram of the times between the photon pulses is shown in fig. 34. No afterpulsing was found in the R5900-L16. It appears unlikely that the absence of afterpulses was a special feature of the tested device. The result is surprising because afterpulsing is detectable in all PMTs of conventional design. It seems that the ‘metal channel’ design of the R5900 is really different from any conventional dynode structure. That means, the R5900-L16 and the PML-16 detector head are exceptionally suitable for combined multi-wavelength fluorescence lifetime and FCS experiments. The absence of afterpulses can be a benefit also in high repetition rate TCSPC measurements in that there is no signal-dependent background. A R5900-L16 with a GaAs or GaAsP cathode - although not announced yet - would be a great detector.

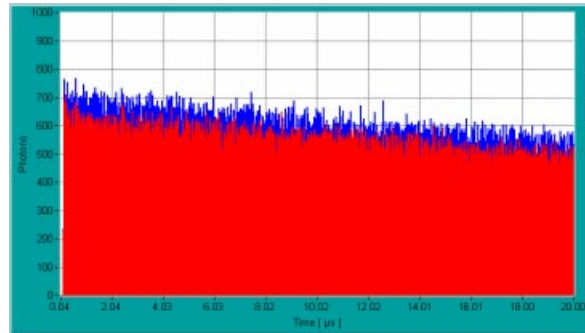


Fig. 34: R5900-L16, histogram of times between photons. No afterpulsing was found.

Side Window PMTs

Side window PMTs are rugged, inexpensive, and often have somewhat higher cathode efficiency than front window PMTs. The broad TTS and the long SER pulses make them less useful for TCSPC application or for multiscaling or gated photon counting with high peak count rates. However, side-window PMTs are used in many fluorescence spectrometers, in femtosecond correlators and in laser scanning microscopes. If an instrument like these has to be upgraded with a photon counting device it can be difficult to replace the detector. Therefore, some typical results for side window PMTs are given below.

The width and the shape of the TCSPC system response depend on the size and the location of the illuminated spot on the photocathode. The response for the R931 - a traditional 28 mm diameter PMT - for a spot diameter of 3 mm is shown in Fig. 35.

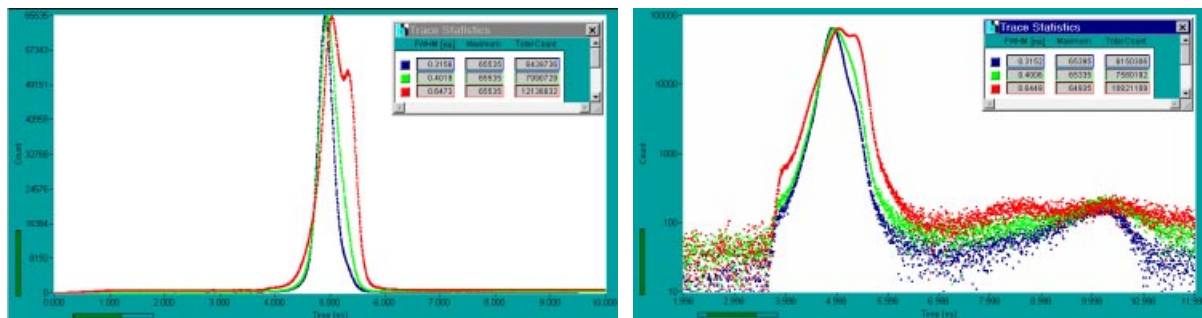


Fig. 35: R931, TCSPC system response for different spots on the photocathode. Spot diameter 3mm

By carefully selecting the spot on the photocathode an acceptable response can be achieved [31,32]. A TCSPC response width down to 112 ps FWHM has been reported [32]. This short value was obtained by using single electron pulses in an extremely narrow amplitude interval and illuminating a small spot near the edge of the cathode.

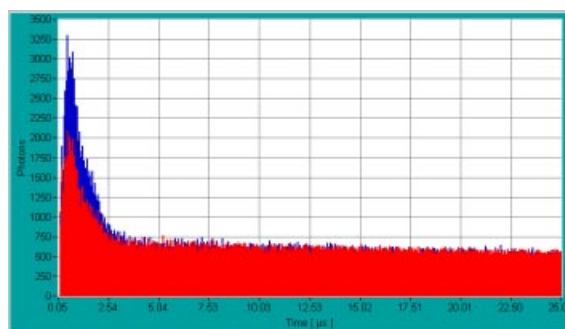


Fig. 36: R931, histogram of times between photons. Red -900V, blue -1000V. The afterpulse probability increases with voltage

The afterpulse probability for an R931 is shown in Fig. 36. The afterpulse probability depends on the operating voltage, and the afterpulses occur within a time interval of about 3 μ s. The high afterpulse probability does not only exclude correlation measurements on the time scale below 3 μ s, it can also result in a considerable signal-dependent background in high repetition rate TCSPC applications.

Surprisingly, modern 13 mm diameter side window tubes are not faster than the traditional 28 mm tubes. The TCSPC response for a Hamamatsu R6350 is shown in fig. 37.

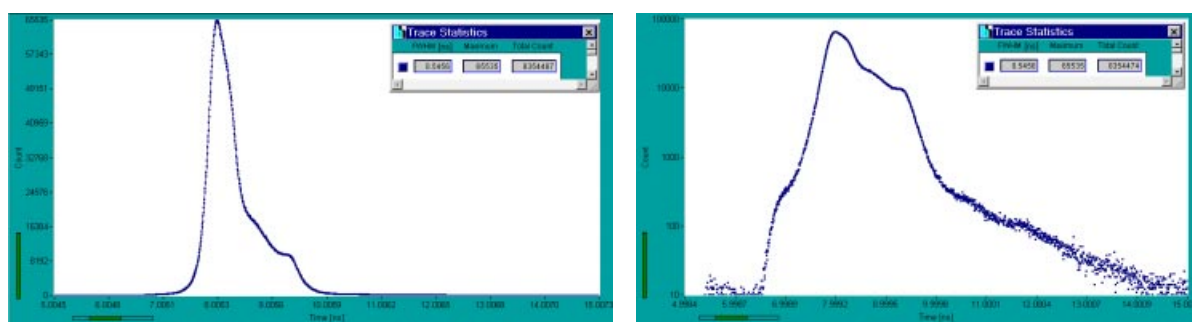


Fig. 37: R6350, TCSPC system response for illumination of full cathode area

13 mm tubes are often used in the scanning heads of laser scanning microscopes. It is difficult, if not impossible to replace the side-window PMTs with faster detectors in these instruments. Therefore it is often unavoidable to use the 13 mm side-on tube for TCSPC lifetime imaging. Depending on the size and the location of the illuminated spot an FWHM of 300 to 600 ps can be expected. Although this is sufficient to determine the lifetimes of typical high quantum yield chromophores, accurate FRET and fluorescence quenching experiments require a higher time resolution.

CP 944 Channel Photomultiplier

The channel photomultipliers of Perkin Elmer offer high gain and low dark count rates at a reasonable cost. Unfortunately the devices have an extremely broad TTS. The TCSPC system response to a 650nm diode laser is shown in fig. 38. The FWHM of the response is of the order of 1.4 to 1.9 ns which is insufficient for typical TCSPC applications.

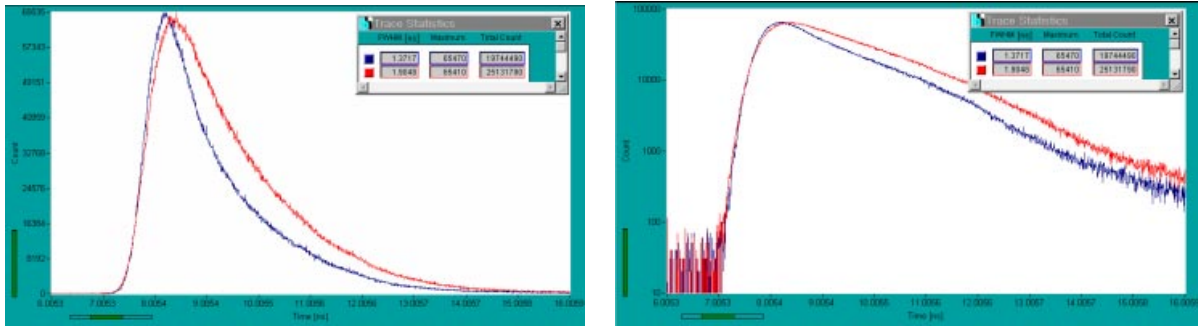


Fig. 38: CP 944 channel photomultiplier, TCSPC response. 650 nm, count rate 1.5.10⁵, high voltage -2.8 kV (red) and -2.9 kV (blue). Full cathode illuminated

However, the Perkin Elmer channel PMTs have high gain, a low dark count rate and a surprisingly narrow pulse height distribution. This makes them exceptionally useful for low intensity steady state photon counting or multichannel scaling.

SPCM-AQR Single Photon Avalanche Photodiode Module

The Perkin Elmer SPCM-AQR single photon avalanche photodiode modules are well-known for their high quantum efficiency in the near-infrared. Unfortunately the modules have a very poor timing performance. The TCSPC response for a SPCM-AQR-12 (dark count class <250 cps) is shown in fig. 39.

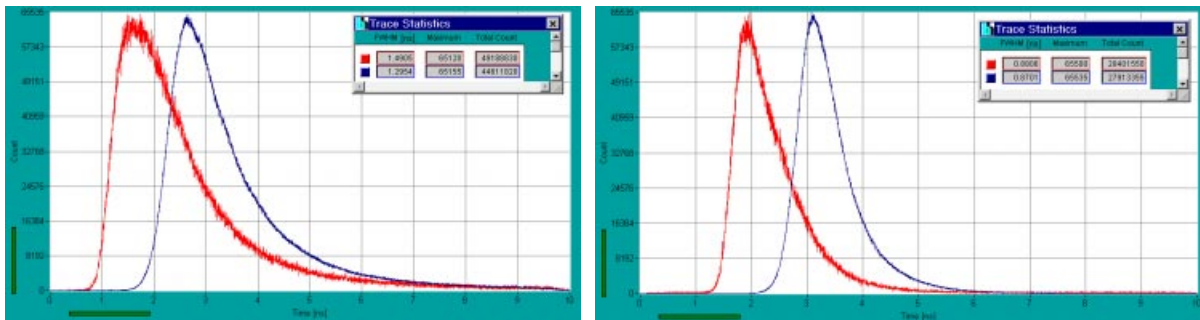


Fig. 39: SPCM-AQR-12, TCSPC response. Left: 405nm, red 50 kHz, blue 500 kHz count rate. Right: 650 nm, red 50 kHz, blue 500 kHz count rate

The response was measured with a 405 nm BDL-405 and a 650 nm ps diode laser of Becker & Hickl. The pulse width of the lasers was 70 to 80 ps, i.e. much shorter than the detector response. The measurements show that the TTS is not only much wider than specified, there is also a considerable change with the wavelength, and, still worse, with the count rate. Therefore the SPCM-AQR cannot be used for fluorescence lifetime measurements.

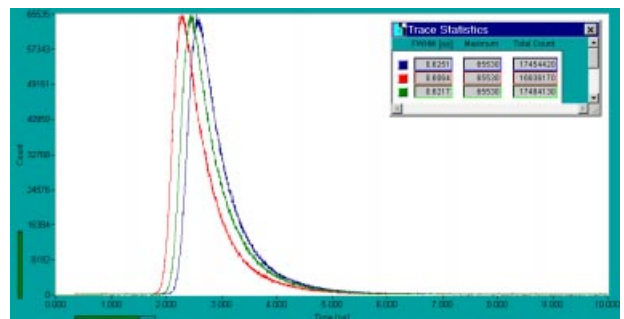


Fig. 40: SPCM-AQR-14, 650 nm, count rates $8 \cdot 10^4$ (green), $5 \cdot 10^5$ (red) and $1 \cdot 10^6$ (blue)

Interestingly, an older SPCM-AQR had a smaller count-rate dependence. Fig. 40 shows the TCSPC response of an SPCM-AQR-14 (dark count class < 40 cps) manufactured in 1999. Although the shift with the count rate is still too large for fluorescence lifetime experiments, it is much smaller than for the new device.

The afterpulse probability of the SPCM-AQR is low enough for correlation experiments down to a few 100 ns, fig. 41.

An inconvenience of the non-fibre version of the SPCM-AQR is that it is almost impossible to attach it to an optical system without getting daylight into the optical path. A standard optical adapter, e.g. a C-mount thread around the photodiode, would simplify the optical setup considerably.

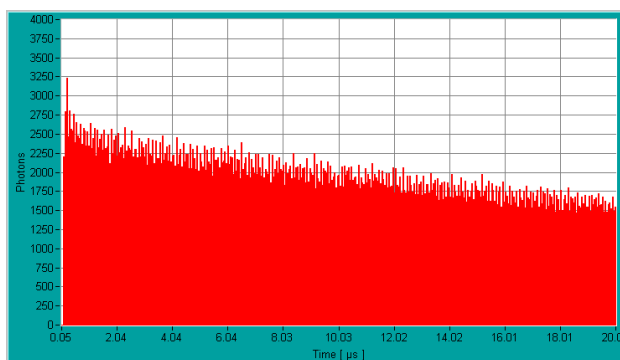


Fig. 419: SPCM-AQR-12, histogram of times between photons

The conclusion is that the SPCM-AQR is an excellent detector for fluorescence correlation spectroscopy and high efficiency steady state photon counting but not applicable to fluorescence lifetime measurements. This is disappointing, particularly because state-of-the-art TCSPC techniques allow for simultaneous FCS / lifetime measurements which are exceptionally useful to investigate conformational changes in protein-dye complexes, single-molecule FRET and diffusion processes in living cells. Currently the only solution for these applications is to use PMT detectors, i.e. the R3809U MCP, the H7422 or the R5900 which, of course, means to sacrifice some efficiency.

Summary

There is no detector that meets all requirements of photon counting - high quantum efficiency, low dark count rate, short transit time spread, narrow pulse height distribution, high peak count rate, high continuous count rate, and low afterpulse probability. The detector with the highest efficiency, the Perkin Elmer SPCM-AQR, has a broad and count-rate dependent transit time spread. The R7400 miniature PMTs and the H5783 and H5773 photosensor modules of Hamamatsu have a short transit-time spread and work well for TCSPC, steady state photon counting, and multiscaler applications. However, they cannot be used for correlation experiments below 1.5 μ s because of their high afterpulse probability. The H7422 modules offer high efficiency combined with acceptable transit time spread. The afterpulse probability can be kept low if they are operated at reduced gain.

There are two really remarkable detectors - the Hamamatsu R3809U MCP and the R5900 multi-anode PMT. Both tubes are free of afterpulses. The R3809U achieves a TTS, i.e. a TCSPC response below 30 ps FWHM while the R5900-L1 reaches < 200 ps in 16 parallel channels. Only these detectors appear fully applicable for simultaneous fluorescence correlation and lifetime experiments.

References

- [1] Photomultiplier Tube, Hamamatsu Photonics, 1994
- [2] PMS-400 Gated photon Counter and Multiscaler. 70 pages, Becker & Hickl GmbH, www.becker-hickl.com
- [3] PMM-328 8 Channel Gated Photon Counter / Multiscaler. 62 pages, Becker & Hickl GmbH, www.becker-hickl.com
- [4] E.P. Buurman, R. Sanders, A. Draijer, H.C. Gerritsen, J.J.F. van Veen, P.M. Houpt, Y.K. Levine : Fluorescence lifetime imaging using a confocal laser scanning microscope. *Scanning* 14, 155-159 (1992).
- [5] J. Syrtsma, J.M. Vroom, C.J. de Grauw, H.C. Gerritsen, Time-gated fluorescence lifetime imaging and microvolume spectroscopy using two-photon excitation. *Journal of Microscopy*, 191 (1998) 39-51

- [6] MSA-200, MSA-300, MSA-1000 Ultrafast Photon Counters / Multiscalers. 65 pages, Becker & Hickl GmbH, www.becker-hickl.com
- [7] Model P7886, P7886S, P7886E PCI based GHz Multiscaler. www.fastcomtec.com
- [8] D.V. O'Connor, D. Phillips, Time Correlated Single Photon Counting, Academic Press, London 1984
- [9] SPC-134 through SPC-830 operating manual and TCSPC compendium. 186 pages, Becker & Hickl GmbH, Jan. 2002, www.becker-hickl.com
- [10] Ballew, R.M., Demas, J.N., An error analysis of the rapid lifetime determination method for the evaluation of single exponential decays. *Anal. Chem.* 61 (1989) 30-33
- [11] K. Carlsson, J.P. Philip, Theoretical Investigation of the Signal-to-Noise ratio for different fluorescence lifetime imaging techniques. SPIE Conference 4622A, BIOS 2002, San Jose 2002
- [12] Routing Modules for Time-Correlated Single Photon Counting, Becker & Hickl GmbH, www.becker-hickl.com
- [13] PML-16 16 Channel Detector Head, Operating Manual. Becker & Hickl GmbH, www.becker-hickl.com
- [14] W. Becker, A. Bergmann, H. Wabnitz, D. Grosenick, A. Liebert, High count rate multichannel TCSPC for optical tomography. *Proc. SPIE* 4431, 249-254 (2001), ECBO2001, Munich
- [15] Wolfgang Becker, Axel Bergmann, Christoph Biskup, Thomas Zimmer, Nikolaj Klöcker, Klaus Benndorf, Multi-wavelength TCSPC lifetime imaging. *Proc. SPIE* 4620, BIOS 2002, San Jose
- [16] Wolfgang Becker, Klaus Benndorf, Axel Bergmann, Christoph Biskup, Karsten König, Uday Tirupapur, Thomas Zimmer, FRET Measurements by TCSPC Laser Scanning Microscopy, *Proc. SPIE* 4431, ECBO2001, Munich
- [17] J. Schaffer, A. Volkmer, C. Eggeling, V. Subramaniam, C. A. M. Seidel, Identification of single molecules in aqueous solution by time-resolved anisotropy. *Journal of Physical Chemistry A*, 103 (1999) 331-335
- [18] TCSPC Laser Scanning Microscopy - Upgrading laser scanning microscopes with the SPC-830 and SPC-730 TCSPC lifetime imaging modules. 36 pages, Becker&Hickl GmbH, www.becker-hickl.com
- [19] K.M. Berland, P.T.C. So, E. Gratton, Two-photon fluorescence correlation spectroscopy: Method and application to the intracellular environment. *Biophys. J.* 88 (1995) 694-701
- [20] P. Schwille, S. Kummer, A.H. Heikal, W.E. Moerner, W.W. Webb, Fluorescence correlation spectroscopy reveals fast optical excitation-driven intramolecular dynamics of yellow fluorescent proteins. *PNAS* 97 (2000) 151-156
- [21] Michael Prummer, Christian Hübner, Beate Sick, Bert Hecht, Alois Renn, Urs P. Wild, Single-Molecule Identification by Spectrally and Time-Resolved Fluorescence Detection. *Anal. Chem.* 2000, 72, 433-447
- [22] W. Hartmann, F. Bernhard, Fotovervielfacher und ihre Anwendung in der Kernphysik. Akademie-Verlag Berlin 1957
- [23] S. Cova, S. Lacaiti, M. Ghioni, G. Ripamonti, T.A. Louis, 20-ps timing resolution with single-photon avalanche photodiodes. *Rev. Sci. Instrum.* 60, 1989, 1104-1110
- [24] S. Cova, A. Longoni, G. Ripamonti, Active-quenching and gating circuits for single-photon avalanche diodes (SPADs). *IEEE Trans. Nucl. Science*, NS29 (1982) 599-601
- [25] P.A. Ekstrom, Triggered-avalanche detection of optical photons. *J. Appl. Phys.* 52 (1981) 6974-6979
- [26] SPCM-AQR Series, www.perkin-elmer.com
- [27] R3809U MCP-PMT, Hamamatsu data sheet. www.hamamatsu.com
- [28] H7422 Photosensor modules. www.hamamatsu.com
- [29] Wolfgang Becker, Axel Bergmann, Georg Weiss, Lifetime Imaging with the Zeiss LSM-510. *Proc. SPIE* 4620, BIOS 2002, San Jose
- [30] H5783 and H5773 photosensor modules. www.hamamatsu.com
- [31] Rinaldo Cubeddu, Eleonora Giambattistelli, Antonio Pifferi, Paola Taroni, Alessandro Torricelli, Portable 8-channel time-resolved optical imager for functional studies of biological tissues, *Proc. SPIE*, 4431, 260-265

- [32] S. Kinishita, T. Kushida, High-performance, time-correlated single-photon counting apparatus using a side-on type photomultiplier, *Rev. Sci. Instrum.* 53, 1983, 469-475
- [33] S. Canonica, J. Forrer, U.P. Wild, Improved timing resolution using small side-on photomultipliers in single photon counting, *Rev. Sci. Instrum.* 56, 1985, 1754- 1785